Journal of Crystal Growth ∎ (∎∎∎∎) ∎∎∎–∎∎∎

Contents lists available at ScienceDirect

Journal of Crystal Growth

journal homepage: www.elsevier.com/locate/jcrysgro

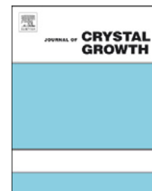

Approach for dislocation free GaN epitaxy

J.K. Hite *, M.A. Mastro, C.R. Eddy Jr.

Naval Research Laboratory, Code 6882, 4555 Overlook Ave, SW, Washington, DC 20375, USA

ARTICLE INFO

Article history:
Received 20 April 2010
Received in revised form
20 July 2010
Accepted 22 July 2010
Communicated by M.S. Goorsky

Keywords:
A1. Defect reduction
A1. Electron channeling contrast imaging
A3. Metalorganic chemical vapor deposition
A3. Selective epitaxy
B1. Gallium Nitride
B2. Semiconducting III–V materials

ABSTRACT

The characteristics of confined epitaxial growth are investigated with the goal of determining the contributing effects of mask attributes (spacing, feature size) and growth conditions (V/III ratio, pressure, temperature) on the efficiency of the approach for dislocation density reduction of GaN. In addition to standard (secondary electron and atomic force) microscopy, electron channeling contrast imaging (ECCI) is employed to identify extended defects over large (tens of microns) areas. Using this method, it is illustrated that by confining the epitaxial growth, high quality GaN can be grown with dislocation densities approaching zero.

© 2010 Elsevier B.V. All rights reserved.

1. Introduction

Wide band gap III-nitride semiconductors are the dominant material for the blue and green optoelectronic industry as well as entering the market as lateral high power and frequency devices. However, in GaN-based devices there are significant prospects of using vertically conducting devices in high power and temperature applications. Due to heteroepitaxial growth limits within this system, high densities of extended defects such as threading dislocations arise, inhibiting the full potential of both optical and electronic devices with vertical currents. Several growth approaches (epitaxial lateral overgrowth (ELO), pendeoepitaxy, etc.) have attempted to minimize the effects of the high defect density in III-N devices [1–5]. For use in vertical devices, though, these growth approaches fail to provide vertical current flow involving the substrate and make poor use of the substrate area impacting yield. Recent research developing a form of selective growth, termed confined epitaxy (CE), has shown materials with dislocation densities reduced by a factor of 10 and stress reductions of 50% compared with continuous layers [6,7]. Unlike LEO and pendeoepitaxy, this approach does not employ lateral growth or re-growth as the basis of defect reduction. Instead, overgrowth is discouraged in the growth and the final product consists of columns of low dislocation GaN. The material improvements are theorized to be the result of the ability of the confined epitaxy columns to twist and flex to accommodate strain without a need for extended defect formation [8]. Taking advantage of the improved material, two-color UV imagers have been fabricated using this approach [9].

In this paper, the characteristics of the CE method will be more fully investigated with the goal of determining the contributing effects of mask attributes (spacing, feature size) and growth conditions (V/III ratio, pressure, temperature) on the efficiency of dislocation density reduction. In order to effectively monitor dislocation density, a rapid, non-destructive method of characterization is preferred. In this work electron channeling contrast imaging (ECCI) is employed to identify extended defects over large (tens of microns) areas. ECCI provides a way to fingerprint threading dislocation number and type within GaN by examining them at their point of intersection with the surface. The technique also permits highlighting of atomic step morphologies and low-angle grain boundaries, and can even be employed to determine the burgers vector of dislocations [10,11].

2. Experimental details

The details to this growth method and its preparation have been previously noted by Eddy et al. [6]. In short, an a-plane sapphire wafer with a 25 nm AlN buffer layer and a 1–2 μm GaN epilayer grown via metalorganic chemical vapor deposition (MOCVD) is patterned via lift-off photolithography and oxide deposition. The resulting 500 nm SiO_x mask on the surface of the

* Corresponding author. Tel.: +1 202 404 8713; fax: +1 202 404 4071.
E-mail address: jennifer.hite.ctr@nrl.navy.mil (J.K. Hite).

0022-0248/$ - see front matter © 2010 Elsevier B.V. All rights reserved.
doi:10.1016/j.jcrysgro.2010.07.054

Please cite this article as: J.K. Hite, et al., J. Crystal Growth (2010), doi:10.1016/j.jcrysgro.2010.07.054

Report Documentation Page

Form Approved
OMB No. 0704-0188

Public reporting burden for the collection of information is estimated to average 1 hour per response, including the time for reviewing instructions, searching existing data sources, gathering and maintaining the data needed, and completing and reviewing the collection of information. Send comments regarding this burden estimate or any other aspect of this collection of information, including suggestions for reducing this burden, to Washington Headquarters Services, Directorate for Information Operations and Reports, 1215 Jefferson Davis Highway, Suite 1204, Arlington VA 22202-4302. Respondents should be aware that notwithstanding any other provision of law, no person shall be subject to a penalty for failing to comply with a collection of information if it does not display a currently valid OMB control number.

1. REPORT DATE	2. REPORT TYPE	3. DATES COVERED
20 JUL 2010		**00-00-2010 to 00-00-2010**

4. TITLE AND SUBTITLE	
Approach for dislocation free GaN epitaxy	5a. CONTRACT NUMBER
	5b. GRANT NUMBER
	5c. PROGRAM ELEMENT NUMBER
6. AUTHOR(S)	5d. PROJECT NUMBER
	5e. TASK NUMBER
	5f. WORK UNIT NUMBER
7. PERFORMING ORGANIZATION NAME(S) AND ADDRESS(ES) **Naval Research Laboratory,Code 6882,4555 Overlook Ave, SW,Washington,DC,20375**	8. PERFORMING ORGANIZATION REPORT NUMBER
9. SPONSORING/MONITORING AGENCY NAME(S) AND ADDRESS(ES)	10. SPONSOR/MONITOR'S ACRONYM(S)
	11. SPONSOR/MONITOR'S REPORT NUMBER(S)

12. DISTRIBUTION/AVAILABILITY STATEMENT

Approved for public release; distribution unlimited

13. SUPPLEMENTARY NOTES

14. ABSTRACT

The characteristicsofconfinedepitaxialgrowthareinvestigatedwiththegoalofdeterminingthe contributingeffectsofmaskattributes(spacing,featuresize)andgrowthconditions(V/IIIratio pressure,temperature)ontheefficiencyoftheapproachfordislocationdensityreductionofGaN.In additiontostandard(secondaryelectronandatomicforce)microscopy,electronchannelingcontrast imaging(ECCI)isemployedtoidentifyextendeddefectsoverlarge(tensofmicrons)areas.Usingthis method,itisillustratedthatbyconfiningtheepitaxialgrowth,highqualityGaNcanbegrownwith dislocationdensitiesapproachingzero.

15. SUBJECT TERMS

16. SECURITY CLASSIFICATION OF:			17. LIMITATION OF ABSTRACT	18. NUMBER OF PAGES	19a. NAME OF RESPONSIBLE PERSON
a. REPORT	b. ABSTRACT	c. THIS PAGE			
unclassified	**unclassified**	**unclassified**	**Same as Report (SAR)**	**4**	

Standard Form 298 (Rev. 8-98)
Prescribed by ANSI Std Z39-18

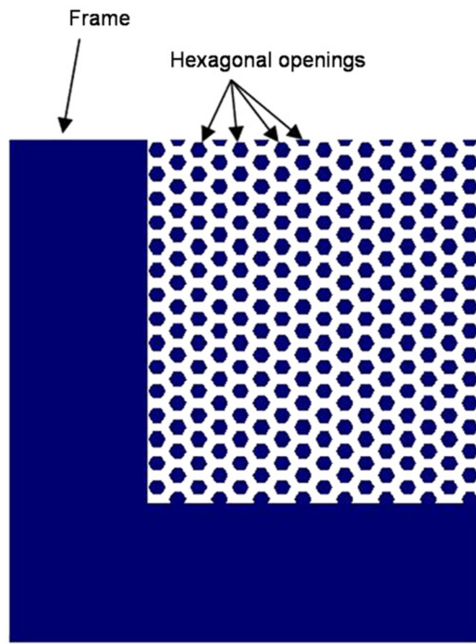

Fig. 1. Magnified view of of the corner of a 20 μm array with 15 μm spacing between features. The white regions are covered by an oxide mask, and the colored areas are the regions left open for GaN growth. Both "frame" and hexagonal openings are visible.

epitaxy consists of hexagonal openings in which the confined epitaxy is grown. The epitaxy is grown only within the openings of the mask, and is not encouraged to expand laterally over the mask. In this study, the opening size is varied between 5 and 20 μm and the spacing between the openings varies between 3 and 15 μm. Variations in process conditions are also examined. In addition, a "border" or "frame" with a 200 μm width was added around each CE array to provide "large area" epitaxial openings. This frame acts like a gallium sink, preventing lateral diffusion across the mask periphery into the edges of the array, which would lead to wide variations in growth rate. An added benefit of this frame is that it allows comparison between large area growth and confined growth under the same local and global conditions. A magnified representation of the corner of an array demonstrating the layout of the hexagonal openings and frame is contained in Fig. 1. The conditions investigated in the MOCVD chamber during the growth included V/III ratios from 500 to 9000, growth temperatures from 1000 to 1100 °C, and pressures from 60 to 250 Torr. The default conditions were 150 Torr, a V/III ratio of 3500, 24.85 μmol/min TMG, and 1030 °C.

Morphological characterization of the CE material was performed by scanning electron microscopy (SEM, LEO Supra 55 SEM) and atomic force microscopy (AFM) in tapping mode (Digital Instruments Nanoscope IIIa). The structural quality of the films and dislocation density was determined by ECCI, using a FEI Nova 600 NanoLab SEM and hkl Technology Nordlys electron backscatter diffraction (EBSD) detector. This characterization method has been shown to pinpoint dislocations and distinguish between edge and screw/mixed dislocations as effectively as transmission electron microscopy (TEM) in both GaN and SiC materials [10,12].

3. Results and discussion

SEM and AFM of the CE columns reveal smooth surfaces for all growth conditions and mask configurations investigated, with rms roughness values similar to that of comparable continuous GaN epilayers (0.4 ± 0.2 nm). Some lateral overgrowth was observed, especially under high V/III conditions, as is commonly seen in two-step LEO growths [13]. In general, vertical sidewalls were not obtained; instead a sidewall with roughly 62° was observed, which corresponds to the (1 −1 0 1) plane. However, at a global V/III ratio of 1500, some 5 μm arrays showed columns with partial vertical sidewalls, but only at the edge of the array. This is most likely a result of an increase in the local V/III, as less Ga is available, and was not duplicated globally. LEO growth observations support this idea, as under low V/III conditions the slope of the initial sidewalls convert to vertical, but only after overgrowing the mask [14]. At MOCVD growth temperatures, the sticking coefficient of Ga on GaN and SiO_x is ~1 and ~0, respectively [15]. Even while using low global V/III ratios with the LEO method, the lateral growth reduces the distance between features, decreasing the additional Ga flux over the mask so that the *local* V/III increases [16].

In general growth trends, the CE column growth rate increased with both increase in spacing and decrease in feature size. This was expected due to lateral diffusion of active species (Ga) over the SiO_x mask within the array. In addition, the growth rate varied between the edge and center of the arrays. This is presumed to be the result of local V/III ratio variations at the edge of the array due to the frame geometry. These effects are illustrated in Fig. 2. The effect diminishes with larger feature sizes, as shown in a more uniform growth rate across individual 20 μm arrays. The edge of the array frame also experiences a higher growth rate. Reducing the V/III ratio naturally increased total growth rates, and during this study growth rates reached as high as 12 μm/hr, far more than conventional, full-wafer growth rates under these same conditions (~2 μm/hr).

Fig. 3 illustrates the general appearance of an ECCI image of the top of a CE GaN column. In this image, threading screw/mixed dislocations are indicated as pinpoints of strong light/dark contrast, examples of which are shown in boxes. Characteristic threading edge dislocations have been circled. Small angle grain boundaries can also be observed from the large area contrast and representative areas are denoted with a dotted line. Note the

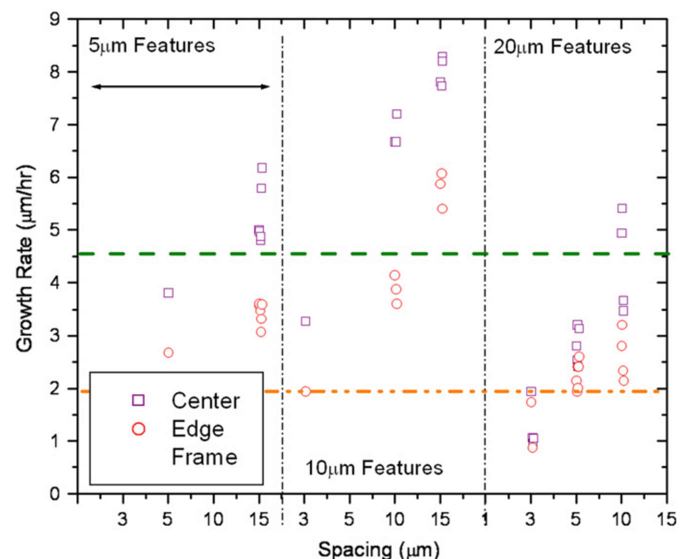

Fig. 2. Growth rate vs. array spacing, feature size, and position within array. Illustrates the enhanced growth rate achieved in CE and the effect the frame has on growth rate at the CE array edge. The line at almost 2 μm/hr represents the growth at the frame center, while that at 4.5 μm/h is an average of the growth rate of the frame edge across multiple arrays.

ARTICLE IN PRESS

threading edge dislocations normally appear at these boundaries as expected.

The ECCI images in Fig. 4a–d illustrate the remarkable reduction in dislocation density achievable with the CE approach. In this, and several other growths, arrays were produced with a majority of columns possessing 0–5 dislocations (corresponding to a maximum dislocation density of 5×10^{7} cm^{-2} for a column surface area of 10 μm^2). Comparing the frame growth (triangles) to array growth (squares and circles) in Fig. 4e illustrates the improved reduction with smaller feature sizes. The trend seen in this graph is representative of all growths carried out using this method. Another important observation from these images arises from the very low dislocation densities in the columns, where thicknesses were between 8 and 9 μm, versus the higher defectivity in the thicker frame edge (12.5 μm). It is generally accepted that thicker growth leads to dislocation annihilation, which is the cornerstone behind using thick (>100 μm) HVPE grown material to obtain low dislocation densities (on the order of $10^6/cm^2$) [17]. However, in the case presented here, a lower dislocation density is observed in thinner films. This leads to the conclusion that an alternative mechanism is driving the dislocation reduction in CE grown material, such as that previously theorized [8].

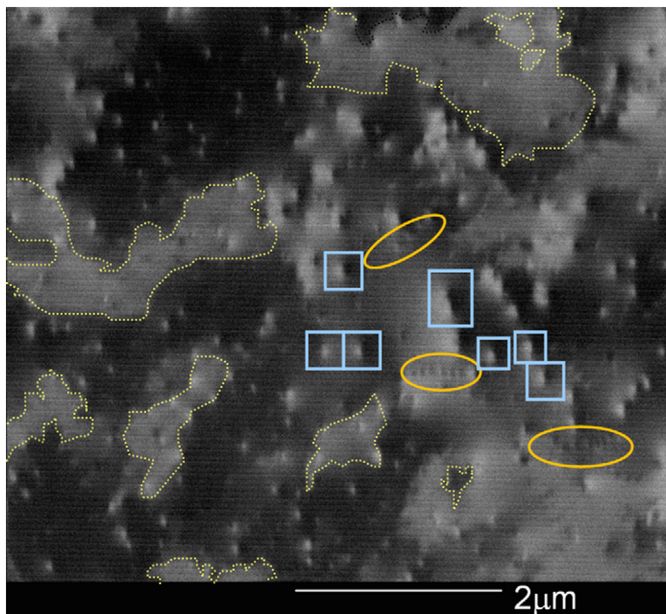

Fig. 3. ECCI Image of GaN CE Column. Threading edge dislocation examples are circled. Examples of threading screw/mixed dislocations are boxed. Examples of small angle grain boundaries are indicated by a dotted line.

According to a theory on the mechanism of dislocation reduction by CE proposed by Twigg et al. [8] a critical thickness is required to allow for the improved dislocation reduction via CE. This is observed in the 10 and 20 μm arrays with thicknesses under 2 μm, shown in Fig. 5b–c. In this case, not only is there a lack of statistical improvement over the frame for the 20 μm features, there is no significant improvement over the underlying epilayer (1.3×10^{9} cm^{-2}). This is observed in Fig. 5e. However, for 5 μm features (Fig. 5a), which were above the critical thickness, the columns show better or equivalent defectivity than the frame edge (Fig. 5d), which was twice as thick. From the reduction in separation from the frame defectivity in the 10 and 20 μm arrays, Fig. 5e demonstrates the need to achieve critical thickness, as previously theorized [8].

The process is robust as other growth parameters had minimal influence on the resulting dislocation density and morphology. If normalized to frame dislocation density and growth thickness, growths for V/III ratios from 500 to 19,000 all show the same trend and relative dislocation density reduction improvement as compared with the frame. The process pressure does play a small role, as at higher pressures (>200 Torr), the CE grown material did not completely fill or form perfect hexagons within the mask openings. Instead, randomly-shaped, pitted columns were formed, which still possess (1 −1 0 1) sidewalls. Changing the growth temperature over the conventional range for MOCVD of III–V nitrides (from 1000 to 1100 °C) did not affect the growth or dislocation reduction process.

4. Conclusion

In conclusion, the major contributing factor to the dislocation density reduction in confined epitaxial growth is the opening size in the mask. In comparing CE growths with larger area frame growth, it is easily determined that the 5 μm features show a drastic reduction in dislocation density, with some arrays

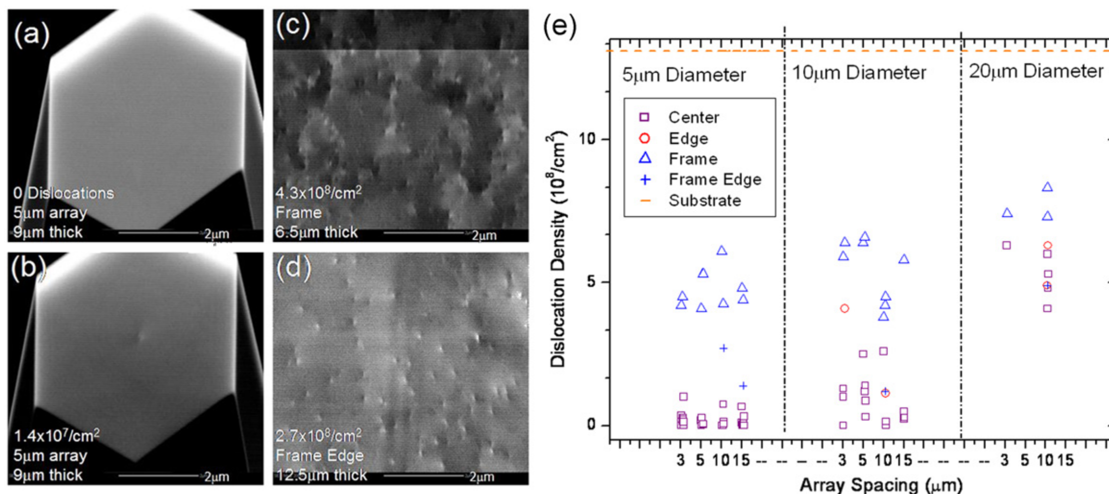

Fig. 4. ECCI images from a 5 μm array showing (a,b) columns with 0 and 1.4×10^{7} dislocations/cm², respectively, (c) frame center with 4.3×10^{8} dislocations/cm², and (d) frame edge with 2.7×10^{8} dislocations/cm². (e) Dislocation density vs. mask properties of spacing, feature diameter, and position in the array. The dotted line at the top represents the dislocation density of the underlying GaN epilayer.

Please cite this article as: J.K. Hite, et al., J. Crystal Growth (2010), doi:10.1016/j.jcrysgro.2010.07.054

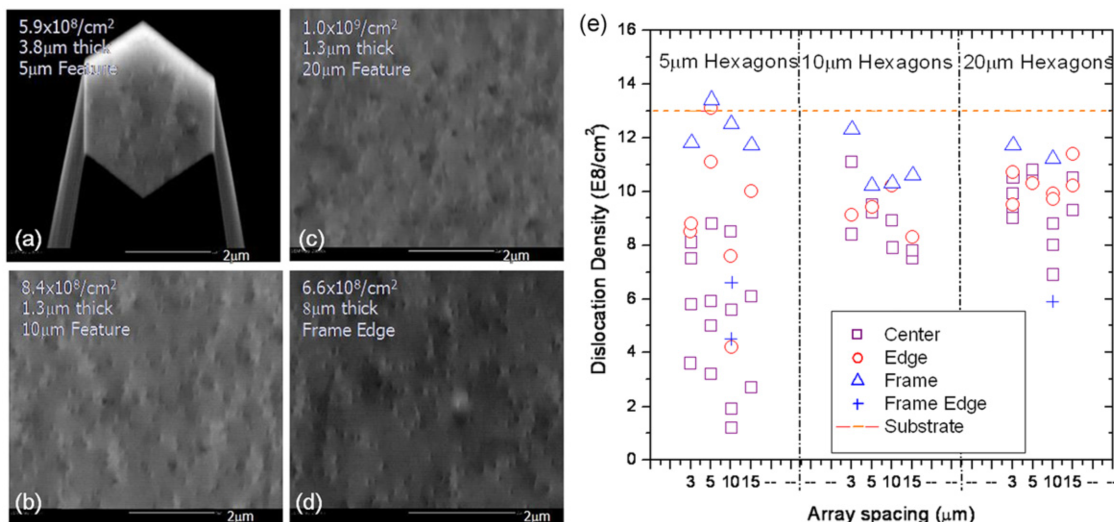

Fig. 5. ECCI images of (a) 5 μm feature 3.8 μm thick with 5.9×10^8 dislocations/cm^2, (b) 10 μm feature 1.3 μm thick with 8.4×10^8 dislocations/cm^2, (c) 20 μm feature 1.3 μm thick with 1.0×10^9 dislocations/cm^2, and (d) frame edge 8 μm thick with 6.6×10^8 dislocations/cm^2. (e) Dislocation density vs. mask properties of spacing, feature diameter, and position in the array. The dotted line at the top represents the dislocation density of the underlying GaN epilayer.

reaching 0 dislocations per column. Also, by comparing the thicker frame growth with CE growth, it is clear that the dislocation reduction in CE is a result of mechanisms other than conventional annihilation. Therefore, the CE method presents the possibility of enabling better vertical devices, which involve the substrate in the device current flow path.

Acknowledgements

This work was supported by the Office of Naval Research. JKH acknowledges the support of the American Society for Engineering Naval Research Laboratory Post-doctoral Fellowship Program. The authors would also like to thank Y.N. Picard and M.E. Twigg for informative conversations on ECCI.

References

[1] T.S. Zheleva, O.-H. Nam, M.D. Bremser, R.F. Davis, Appl. Phys. Lett. 71 (1997) 2472.
[2] D. Kapolnek, S. Keller, R. Vetury, R.D. Underwood, P. Kozodoy, S.P. DenBaars, U.K. Mishra, Appl. Phys. Lett. 71 (1997) 1204.
[3] K. Hiramatsu, K. Nishiyama, M. Onishi, H. Mizutani, M. Narukawa, A. Motogaito, H. Miyake, Y. Iyechika, T. Maeda, J. Cryst. Growth 221 (2000) 316.
[4] K. Linthicum, T. Gehrke, D. Thomson, E. Carlson, P. Rajagopal, T. Smith, D. Batchelor, R. Davis, Appl. Phys. Lett. 75 (1999) 196.
[5] D.M. Follstaedt, P.P. Provencio, N.A. Missert, C.C. Mitchell, D.D. Koleske, A.A. Allerman, C.I.H. Ashby, Appl. Phys. Lett. 81 (2002) 2758.
[6] C.R. Eddy Jr., R.T. Holm, R.L. Henry, M.E. Twigg, N.D. Bassim, L.M. Shirey, O.J. Glembocki, J.C. Culbertson, F.K. Perkins, M.C. Peckerar, Y. Ngu, F. Yan, Appl. Phys. Lett. 90 (2007) 162101.
[7] C.R. Eddy Jr, M.A. Mastro, N.D. Bassim, M.E. Twigg, R.L. Henry, R.T. Holm, J.C. Culbertson, O.J. Glembocki, J.D. Caldwell, P.G. Neudeck, A.J. Trunek, J.A. Powell, M.C. Peckerar, Y. Ngu, F. Yan, S. Babu, ECS Trans. 3 (5) (2006) 117.
[8] M.E. Twigg, N.D. Bassim, C.R. Eddy Jr., R.L. Henry, R.T. Holm, M.A. Mastro, E11.29, Mater. Res. Soc. Symp. Proc. 831 (2005) 1–6.
[9] Y. Ngu, M.C. Peckerar, D. Sander, C.R. Eddy, Jr., M.A. Mastro, J.K. Hite, R.T. Holm, R.L. Henry, A. Tuchman, IEEE Trans. Elect. Devices 56 (2010) 1224.
[10] Y.N. Picard, J.D. Caldwell, M.E. Twigg, C.R. Eddy Jr, M.A. Mastro, R.L. Henry, R.T. Holms, Appl. Phys. Lett. 91 (2007) 094106.
[11] Y.N. Picard, M.E. Twigg, J.D. Caldwell, C.R. Eddy Jr., M.A. Mastro, R.T. Holm, Scr. Mater. 61 (2009) 773.
[12] Y.N. Picard, M.E. Twigg, J.D. Caldwell, C.R. Eddy Jr., P.G. Neudeck, A.J. Trunek, J.A. Powell, Appl. Phys. Lett. 90 (2007) 234101.
[13] B Beaumont, P.H. Vennegues, P. Gibart, Phys. Status Solidi B 227 (2001) 1.
[14] L. Zhang, S.L. Gu, R Zhang, D.M. Hansen, M.P. Boleslawski, T.F. Kuech, J. Cryst. Growth 235 (2002) 115.
[15] T.S. Zheleva, O.-H. Nam, R.F. Davis, in: in: J.H. Edgar, S. Strite, I. Akasaki, H. Amano, C. Wetzel (Eds.), Properties, Processing, and Applications of Gallium Nitride and Related Semiconductors, vol. B2.10, IEE1999, pp. 447–453.
[16] G Feng, Y. Fu, J.S. Xia, J.J. Zhu, B.S. Zhang, X.M. Shen, D.G. Zhao, H. Yang, J.W. Liang., J. Phys. D: Appl. Phys. B 35 (2002) 2731.
[17] S.K. Mathis, A.E. Romanov, L.F. Chen, G.E. Beltz, W. Pompe, J.S. Speck, Phys. Status Solidi A 179 (2000) 125.

Please cite this article as: J.K. Hite, et al., J. Crystal Growth (2010), doi:10.1016/j.jcrysgro.2010.07.054